Geology of the Matthew Creek metamorphic zone, southeast British Columbia: a window into Middle Proterozoic metamorphism in the Purcell Basin

C.R.M. McFarlane and D.R.M. Pattison

Abstract: Southwest of Kimberley, southeastern British Columbia, the Matthew Creek metamorphic zone occupies the core of a structural dome in Mesoproterozoic rocks of the Lower Aldridge formation (lower Purcell Supergroup). It comprises (1) a core zone of ductilely deformed sillimanite-grade metapelites, thin foliated mafic sills, and sheared quartz–plagioclase–tourmaline pegmatites; and (2) a thin transition zone of ductilely deformed metasediments which marks a textural and metamorphic transition between the core zone and overlying regionally extensive, brittlely deformed, biotite-grade semipelitic Lower Aldridge formation metasediments and thick Moyie sills. The core zone and transition zone in combination cover an area of 30 km^2. The deepest exposed rocks in the core zone have a strong foliation and lineation (D_1 deformation) formed during late M_1 metamorphism at conditions of 580–650°C and 3.5 ± 0.5 kbar. The timing of this metamorphic–structural episode is constrained to the interval 1352–1341 Ma based on near-concordant U–Pb ages from monazite in pelitic schist near the mouth of Matthew Creek. Later, weaker metamorphic and deformation episodes variably overprinted the rocks of the Matthew Creek metamorphic zone. The juxtaposition of low-grade, weakly deformed rocks above high-grade, strongly deformed rocks across a zone of ductile deformation is interpreted to be due to a subhorizontal shear zone.

Résumé : Au sud-ouest de Kimberley, dans le sud-est de la Colombie-Britannique, la zone métamorphique de Matthew Creek occupe le centre d'un dôme structural dans des roches mésoprotérozoïques de la Formation d'Aldridge inférieure (Supergroupe de Purcell inférieur). Cette zone métamorphique comprend (1) une zone centrale de métapélites au grade de sillimanite à déformation ductile, de minces filons-couches mafiques foliés et des pegmatites quartz-plagioclase-tourmaline cisaillées et (2) une mince zone de transition de métasédiments à déformation ductile qui marque une transition texturale et métamorphique entre la zone centrale et les roches qui la recouvrent, soit des métasédiments d'Aldridge inférieurs semi-pélitiques, au grade de la biotite, à déformation cassante et d'extension régionale, ainsi que d'épais filons-couches de Moyie. Ensemble, la zone centrale et la zone de transition couvrent une superficie de 30 km^2. Les roches exposées les plus profondes dans la zone centrale ont une forte foliation et une forte linéation (déformation D_1) produites au cours du métamorphisme M_1 tardif, à des températures de 580 à 650 °C et sous des pressions de 3,5 ± 0,5 kbar. Cet épisode métamorphique structural est confié dans le temps à l'intervalle 1352 à 1341 Ma selon des datations U–Pb presque concordantes effectuées sur des monazites dans des schistes pélitiques près de l'embouchure du ruisseau Matthew. Par la suite, des épisodes plus faibles de métamorphisme et de déformation ont surimposé les roches de la zone métamorphique de Matthew Creek. La juxtaposition de roches faiblement déformées à faible métamorphisme par-dessus des roches de haut métamorphisme et fortement déformées à travers une zone de déformation ductile indiquerait une zone de cisaillement sub-horizontale.

[Traduit par la Rédaction]

Introduction

The Matthew Creek metamorphic zone (MCMZ) is one of a few small areas of amphibolite-facies metamorphic rocks that crop out in the Purcell Supergroup sequence in southeastern British Columbia (McMechan and Price 1982). It occupies the core of a structural dome and is surrounded on all sides by the regionally metamorphosed biotite ± garnet-grade metasediments of the lowermost part of the Purcell Supergroup sequence (Lower Aldridge formation) (Fig. 1). One of the most striking features of the MCMZ is the relatively abrupt transition from biotite ± garnet-grade metasediments, showing well-preserved sedimentary features surrounding the MCMZ, to glistening porphyroblastic sillimanite-grade schists within the MCMZ over a vertical distance of less than 1 km. Because the surrounding metasediments are host to the giant Sullivan Pb–Zn mine, 5–6 km to the northeast, there has been considerable geological mapping and mineral exploration surrounding the MCMZ. However, there has been relatively little work done on the MCMZ itself and previous interpretations of its significance are speculative.

Received April 28, 1999. Accepted February 2, 2000.
Published on the NRC Research Press website on July 21, 2000.

C.R.M. McFarlane.[1] Department of Geological Sciences, University of Texas at Austin, Austin, TX 78712–1101, U.S.A.
D.R.M. Pattison. Department of Geology & Geophysics, University of Calgary, Calgary, AB T2N 1N4, Canada.

[1]Corresponding author (e-mail: cmcfarlane@mail.utexas.edu).

Fig. 1. Simplified regional geology and location of the Matthew Creek metamorphic zone with respect to major fold and thrust structures in southeast British Columbia. Modified after Anderson and Parrish.

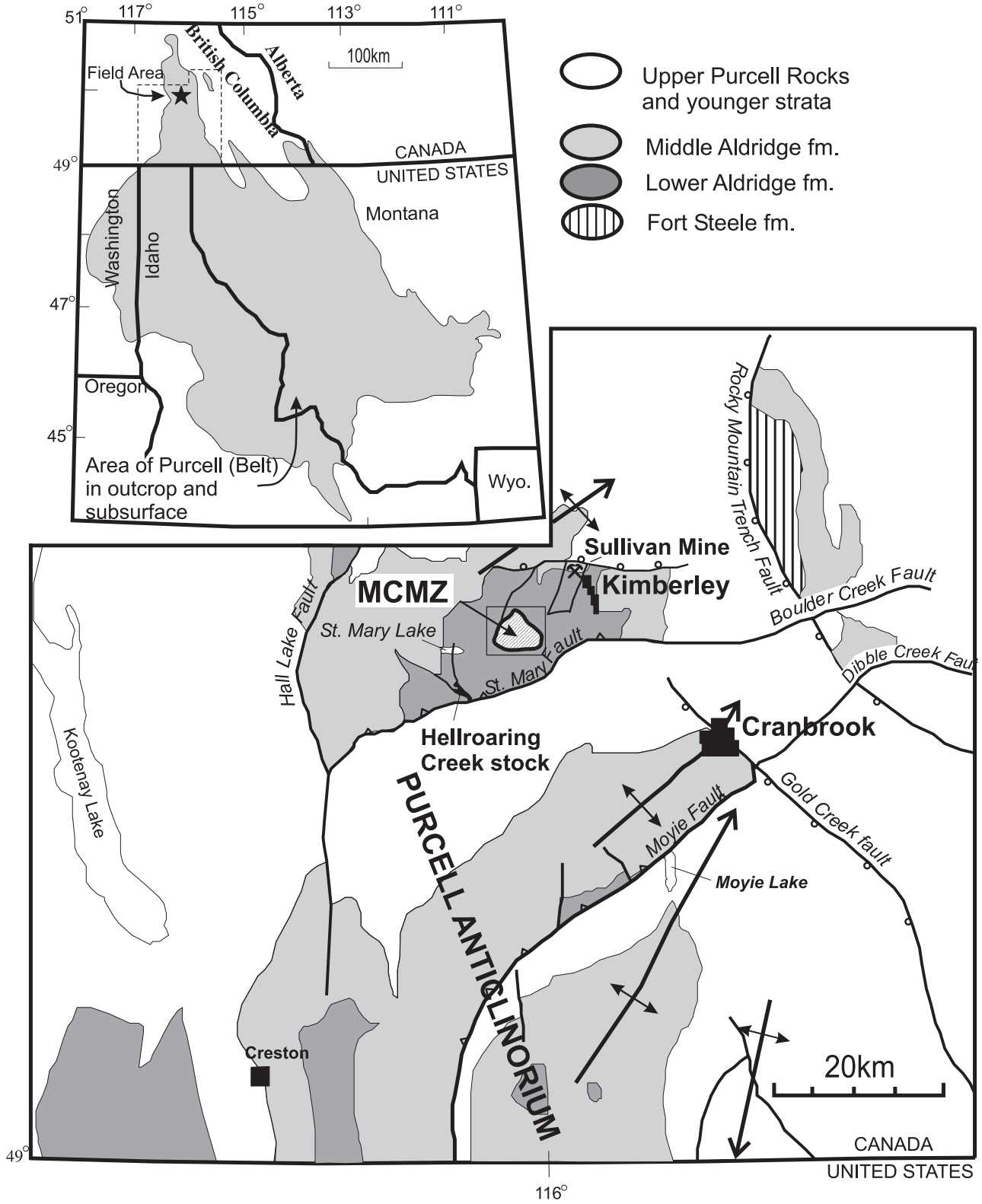

The MCMZ represents a structural window that provides a glimpse into the Proterozoic tectonothermal history of the Purcell Supergroup sequence. Several periods of Middle to Late Proterozoic deformation and metamorphism appear to have affected the lower Purcell Supergroup sequence in this region (Höy et al. 2000), but the details of this early history remain enigmatic. The MCMZ has been widely cited (Leech 1962; Leech et al. 1963; Ryan and Blenkinsop 1971; McMechan and Price 1982; Anderson and Davis 1995) as evidence for a 1320–1360 Ma regional tectonothermal event in the lower Purcell Supergroup sequence, termed the "East Kootenay Orogeny" by White (1959). However, because the MCMZ has never been studied in any systematic way, the significance of its metamorphic and structural features, its relation to the surrounding low-grade Lower Aldridge formation metasediments, and its significance with respect to the Middle Proterozoic tectonothermal evolution of the Purcell Supergroup have remained uncertain. This paper presents the results of detailed mapping and petrological study of the MCMZ and the immediately surrounding metasediments, and speculates on the broader tectonic significance of the MCMZ.

Regional geology

The field area lies on the west side of the Rocky Mountain Trench and on the northern flank of the Purcell Anticlinorium. The rocks consist of Purcell Supergroup metasediments and gabbroic sills, and occur in the hanging wall of the St. Mary Fault, which is exposed roughly 5 km south of the MCMZ. The bulk of the metasediments are Middle Proterozoic (1500–1320? Ma) lower Purcell synrift metasediments of the Aldridge formation (Höy et al. 2000) that are interpreted to have been deposited in a rapidly subsiding sedimentary basin (the Belt–Purcell Basin).

The rocks surrounding the MCMZ belong to the Lower Aldridge formation, the lowermost division of the Purcell Supergroup sequence in the region. In the Kimberley area, the Lower Aldridge formation is a sequence of interbedded argillaceous quartzites and argillites with a characteristic rusty weathering resulting from a high pyrrhotite content. Layer thickness in the Lower Aldridge formation surrounding the MCMZ ranges between <1 cm in argillaceous units to 30 cm in massive quartzite layers. The age of the Lower Aldridge formation is estimated to at least 1468 Ma, based on concordant U–Pb zircon ages (Anderson and Davis 1995) of Moyie sills interpreted to have intruded wet Lower Aldridge formation sediments during an early rifting phase of basin opening (Höy 1989). These laterally extensive sills locally constitute upward of 40% of the stratigraphic column, becoming less abundant up-section and toward the margins of the Belt–Purcell Basin.

Small trondhjemitic stocks that are commonly pegmatitic and rich in muscovite, tourmaline, and beryl also intrude the Aldridge formation. Examples include the Hellroaring Creek stock and the Matthew Creek stock, the latter lying within the MCMZ.

While there is geochronological evidence for Middle Proterozoic metamorphism of the Purcell sequence, the tectonic framework accompanying this metamorphism is uncertain. The dominant structures presently found in the region of the MCMZ are Cordilleran in age, formed as a result of horizontal compression, tectonic thickening, and eastward displacement (possibly accompanied by clockwise rotation (Sears and Price 1994)) over a period of 100 Ma from Late Jurassic to Paleocene time. The Aldridge formation appears to have behaved as a relatively rigid unit and has experienced relatively little internal deformation during this compression, as suggested by the preservation of delicate primary structures in finely laminated, ductile sulphides in the nearby Sullivan orebody.

Metamorphic grade increases with structural depth in the Purcell Basin (McMechan and Price 1982). Garnetiferous Aldridge formation metasediments are widespread although not abundant throughout the region. Idioblastic, Mn-rich garnet-bearing rocks occur in the Sullivan orebody near the transition between Lower and Middle Aldridge formations. DePaoli and Pattison (1995) estimated *P–T* conditions of metamorphism in the Sullivan orebody of 450 ± 50°C and 3.8 ± 1 kbar (1 kbar = 100 MPa) using silicate–carbonate fluid equilibria, and suggested that this metamorphic event correlated with 1322 Ma titanite ages (Schandl et al. 1993) from altered rocks in the Sullivan orebody.

U–Pb age determinations of seven zircon fractions by Anderson and Davis (1995) from four Moyie sills that intrude Middle and Lower Aldridge formation metasediments above the MCMZ in the vicinity of the Sullivan Mine yielded a mean age of 1468 ± 2 Ma, interpreted to be the crystallization age of these sills. A cluster of concordant titanite ages occurs at 1030–1090 Ma. These younger ages may reflect metamorphism in the lower Purcell Supergroup sequence, although structural and petrological evidence for this event remains obscure. No concordant 1320–1370 Ma ages were reported by Anderson and Davis (1995) from these sills, perhaps indicating that the ca. 450°C metamorphic event in the vicinity of the Sullivan orebody (DePaoli and Pattison 1995) was not hot enough to grow metamorphic titanite in the sills. The Cordilleran crustal thickening and tectonism also likely imparted some kind of metamorphic overprint, although this apparently was not strong enough to reset any of the geochemical systems summarized above. To place tighter constraints on the timing of metamorphism in the Purcell Supergroup sequence, further geochronological dating of deformational fabrics and metamorphic minerals will be required.

Previous work and interpretations

Rocks of the MCMZ were first described by S.J. Schofield (1915) and subsequently by Rice (1937) and Leech (1962, 1957), although the full extent of MCMZ was not mapped out. These workers noted the relatively abrupt transition from biotite-grade metasediments showing well preserved sedimentary features outside of the MCMZ to glistening sillimanite-grade schist within the MCMZ. They ascribed this anomalously steep thermal gradient to contact metamorphism during the intrusion of some unexposed granitic body, or to the intrusion of the Matthew Creek stock, which lies within the high-grade core zone. However, there are no geophysical anomalies (National Earth Science Series maps for Kootenay Lake, NM11-GR(BA) 1993, and NM-11 1987) to suggest the presence of such a shallowly buried intrusion, and the contact relationships described here do not support such a hypothesis.

Fig. 2. Generalized geology of the MCMZ showing inferred extents of the transition zone and core zone. Dotted hatching in core zone shows areas of good outcrop exposure.

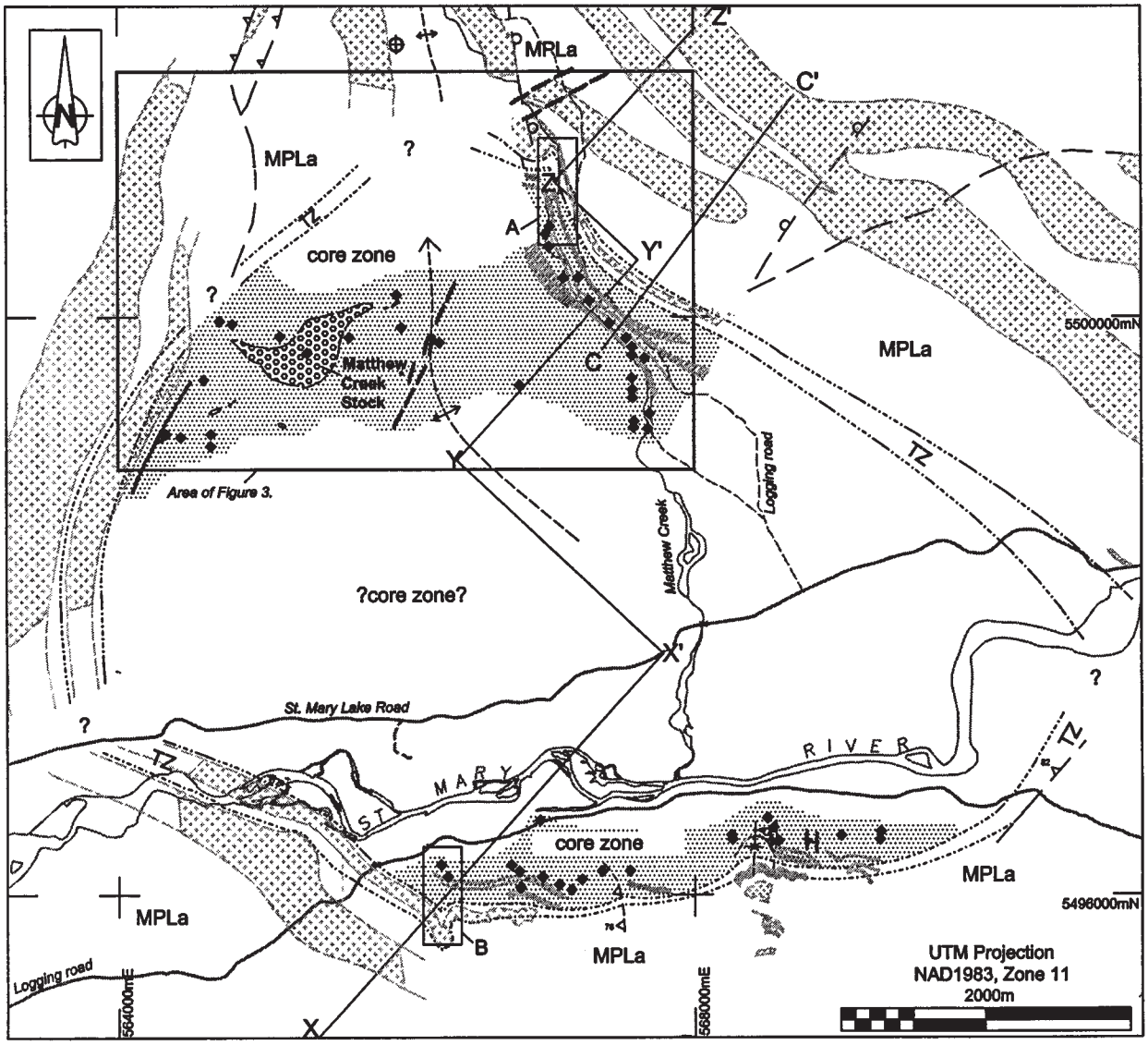

Geology of the Matthew Creek metamorphic zone

The MCMZ occupies the core of a broad dome and can be subdivided into two distinct metamorphic and structural domains (Figs. 2, 3, 4): (1) a core zone of ductilely deformed, coarse-grained, porphyroblastic Grt + Sil schist (abbreviations of Kretz 1983), foliated mafic sills, and deformed pegmatites exposed in the central portion of the dome; and (2) a thin transition zone into the regionally extensive

Fig. 3. Detailed geology of the northern portion of the MCMZ in the vicinity of the Matthew Creek stock. Lithologies as in Fig. 2. Contour interval = 100 m.

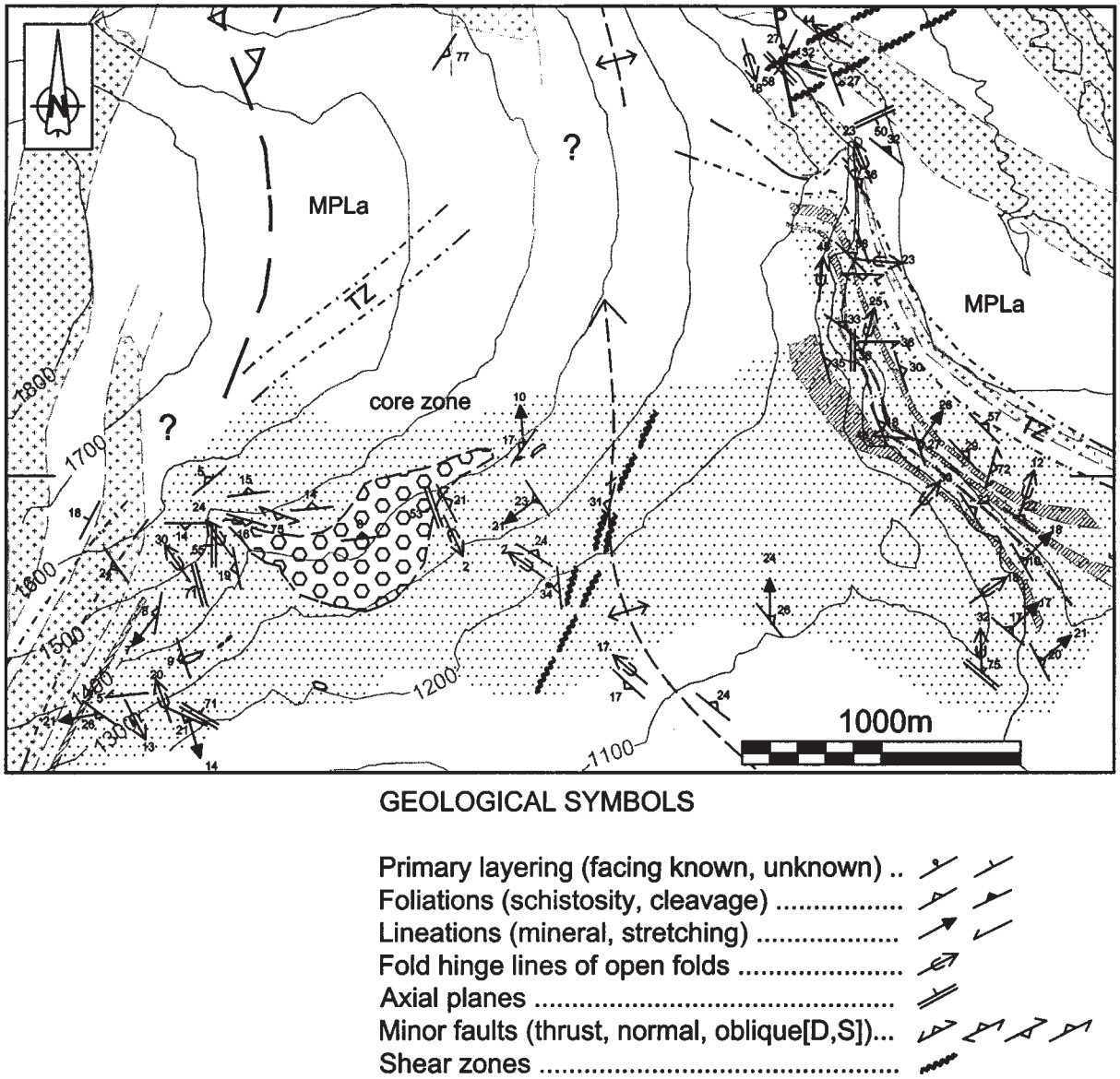

Fig. 4. Schematic cross section along line X–Z′ in Fig. 2. First appearance of sillimanite (sil-in line) is also shown. Lithologies as in Fig. 2.

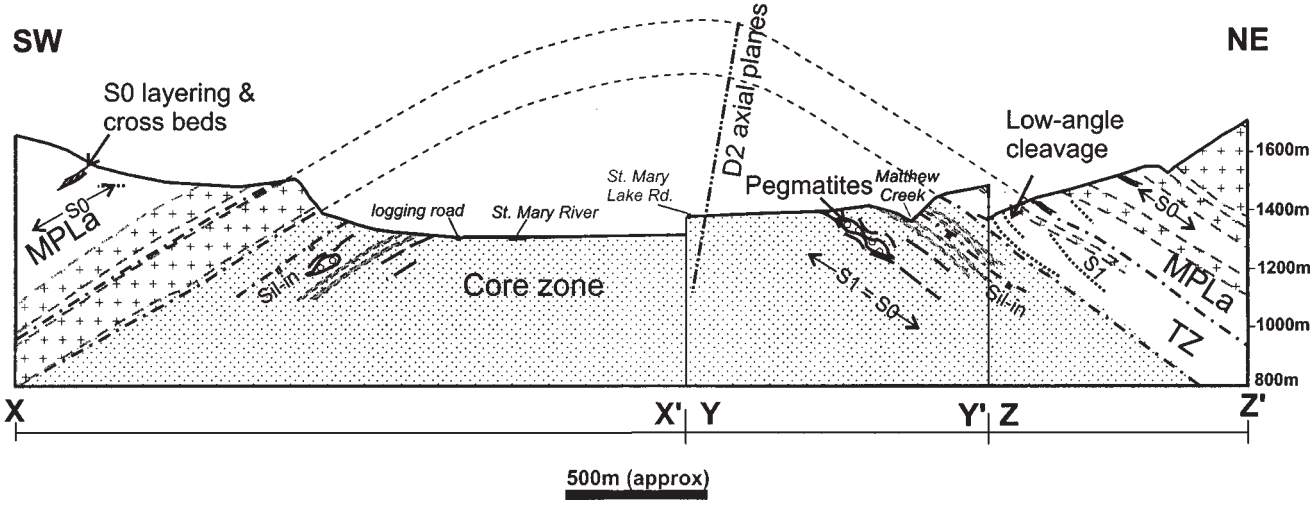

Fig. 5. (A) Siliceous crossbedded regional-grade Lower Aldridge formation. Dark laminations contain a higher proportion of biotite. From the SW corner of the MCMZ roughly 200 m above the core zone (view looking southwest). (B) Ribbed Lower Aldridge formation metasediment roughly 100 m above transition zone in the northwest corner of MCMZ, with well-defined, low-angle cleavage (S_1) and primary sedimentary layering (S_0). (C) Equant Ms_2-rich pseudomorph after andalusite(?) near mouth of Matthew Creek, which deflects the $S_1 = S_0$ schistosity in the core zone. Small dark equant grains are $Grt_{1, 2}$. (D) Lenticular Ms_2-rich pseudomorphs from the same outcrop as (C). Pseudomorphs are present in more pelitic layers sandwiched between thicker siliceous ribs that define the $S_1 = S_0$ foliation in the core zone.

biotite-grade metasediments, consisting of decreasingly foliated fine-grained platy metasediments.

An inherent problem in the study of the MCMZ is the limited and patchy exposure in a heavily tree-covered area. Outcrop covers less than 20% of the map area. The key lithological, petrological, and structural features of the transition zone are only exposed in three main areas: in the steep canyon along Matthew Creek, in steep exposures south of the St. Mary River, and in the vicinity of the Matthew Creek stock. The most serious consequence of the lack of exposure is that some key structural features of the MCMZ could not be determined (see below). Nevertheless, the exposure is sufficient to determine the main lithological, structural, and metamorphic features of the area.

Regional-grade rocks

Metasediments

Lower Aldridge formation metasediments in the surrounding regional-grade rocks are composed of thin (<10 cm) argillaceous layers showing well developed penetrative cleavage interbedded with thicker competent quartzite beds, imparting a ribbed appearance to outcrops. Sedimentary features including crossbedding (Fig. 5A) and grading are well preserved within thicker siliceous beds. Argillaceous layers throughout the Lower Aldridge formation locally display a cleavage S_1 (Fig. 5B), defined by muscovite and biotite, which intersects bedding at 35–60°. In the northeast portion of the field area (see Fig. 3), the low-angle, northeast-dipping cleavage is more steeply dipping than bedding and strikes to the northwest. There is insufficient exposure to assess the orientation of the low-angle cleavage on the southwestern flank of the MCMZ. S_1 cleavage is locally crenulated and the axial planes of this crenulation surface have an orientation similar to the north-trending hinge of the dome that hosts the MCMZ (see Fig. 8). The origin of the early low-angle S_1 cleavage remains uncertain.

Moyie sills

Moyie sills intrude the metasediments and locally comprise upward of 50% of the Lower Aldridge formation sedimentary sequence in the vicinity of the MCMZ. They are dark green, medium- to coarse-grained hypidiomorphic granular rocks with subhedral amphiboles, milky granular plagioclase, fibrous chlorite, and quartz commonly visible in hand sample. Segregations of milky plagioclase and quartz locally impart a blotchy appearance to the rocks. Chilled contacts with metasediments are generally concordant with bedding, and a marked bleaching of metasediments occurs within 50 cm of upper contacts. Sills are generally tabular at the outcrop scale, but pinch and swell and cut across strata unpredictably across the field area.

Core zone

Metapelites

The metapelitic rocks in the core zone are glistening coarse-grained porphyroblastic schists that contrast with the finer grained, rusty-weathering metasediments in the Lower Aldridge formation throughout the region. They contain the mineral assemblage Ms–Bt–Qtz–Pl ± Grt ± Sil ± And ± Cld ± Ilm ± Tur ± Rut (abbreviations of Kretz 1983). About 250 m of stratigraphy is exposed in the core zone. Outcrops display a ribbed appearance defined by alternating layers of friable schistose pelites and more competent quartz-rich semipelites that range in thickness from 1 to 30 cm. These alternating pelitic and siliceous layers are reminiscent of the Lower Aldridge formation argillites and quartz arenites at higher stratigraphic levels. A 5 m thick quartzite unit and several thinner quartzite layers crop out throughout the core zone.

Pelitic schists display a strong sillimanite mineral lineation in the upper portions of the core zone. The 5–30 cm long pseudomorphs rich in coarse, randomly oriented muscovite are ubiquitous throughout the schist. They are randomly oriented within foliations planes, and, in cross section, form squarish (Fig. 5C) to lenticular features strung out parallel to the S_1 foliation (Fig. 5D). The pseudomorphed precursor minerals include andalusite, garnet, and possibly staurolite, based on relic cores of these minerals in the pseudomorphs. Their replacement by randomly oriented muscovite must postdate ductile deformation, since sectile muscovite would not be expected to survive the intense flattening recorded by the elongated porphyroblasts. Coarse lenticular biotite porphyroclasts have cleavages set at a high angle to the S_1 foliation. In thin sections cut perpendicular to S_1 and parallel to L_1 lineations, these large biotites also display quartz inclusion trails that define a fabric (S_0?) that is also set at a high angle to the schistosity. Near the base of this zone, the rocks locally display gneissic banding with concordant quartz–plagioclase–garnet pods oriented parallel to foliation planes.

Metabasites

Mafic sills interlayered with the high-grade schist are generally thin (<10 m thick) and are composed of dark green foliated hornblende with 0.2–1 cm clinozoisite and 1–10 cm garnet porphyroblasts. Many sills display garnet + biotite-rich (10–40%) upper margins. Sills exposed near the base of the exposed core zone also display gneissic banding and contain concordant lenses rich in quartz and plagioclase.

Pegmatites

The core zone contains lenses and pods of pegmatite ranging in thickness from <5 cm to tens of metres. Most of the pegmatite is peraluminous and is composed of plagioclase

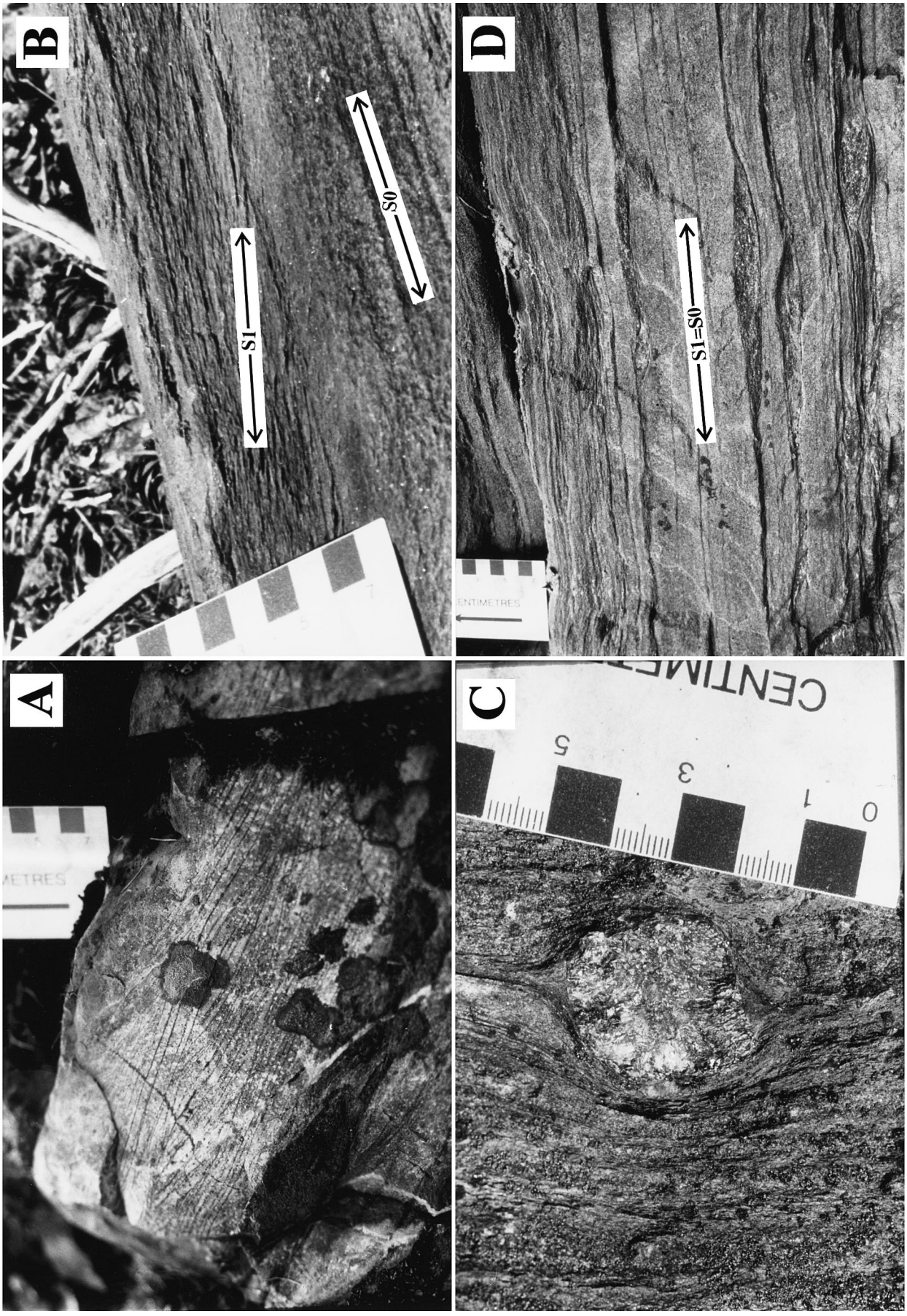

and muscovite with lesser quartz, alkali feldspar and ubiquitous black tourmaline, garnet, and white beryl. The Matthew Creek stock is the largest of these pegmatites (<5 km^2), cropping out in the western portion of the field area. It has a domed roof and an undulatory lower contact, both of which are concordant with the schistosity. All of the pegmatites mapped in the area have deformed margins against the schist. The contacts between the pegmatites and the surrounding schists display a cataclastic fabric defined by fractured feldspars anastomosed by lepidoblastic muscovite that is preserved up to 30 cm into the pegmatites. Many fractured porphyroclasts display domino structures suggesting they have experienced a component of simple shear. Many smaller pegmatitic sills have been boudinaged (Fig. 6A) and transposed into parallelism with the schist. The host rocks adjacent to the pegmatites do not display evidence of contact metamorphism.

Brown tourmalinite layers in schists along the upper contact of several pegmatitic sills (Fig. 6B) suggest that boron-rich metasomatizing fluids may have accompanied their emplacement. The ubiquitous occurrence of tourmaline with green dravitic cores and brown schorl rims throughout the high-grade schist and in the margins of foliated sills suggests that addition of boron-rich fluids to the metamorphic rocks may have been significant and widespread.

Transition zone

The structural and metamorphic changes within the transition zone are gradual, and deformational fabrics are commonly obscured by the effect of late secondary recrystallization. The transition zone is best exposed in rusty weathering fine-grained semipelites along Matthew Creek (location A in Fig. 2), and midway up the north face of the mountainside south of the St. Mary River (location B in Fig. 2). The description below is a synthesis of the continuous sections at localities A and B.

The top of the transition zone is defined by the onset of transposition of the regional cleavage in overlying Lower Aldridge formation semipelites into parallelism with $S_1 = S_0$ foliation in the core zone. The contact between the transition zone and the overlying regional metasediments is, therefore, gradational and difficult to locate precisely. In rocks that look similar to the regional biotite-grade metasediments and that show well-developed primary sedimentary structures, the cleavage intersects S_0 bedding at 10–40°. Transposition to parallelism with S_0 occurs incrementally over the next 100 m of stratigraphy going downward, suggesting that the state of strain varied relatively smoothly as a function of depth towards the core zone. The contact between the transition zone and the underlying core zone schist is placed at the first occurrence of layer-parallel ($S_1 = S_0$) foliations, which is also coincident with the onset of more pelitic schistose rocks.

Identification of the transition zone is further complicated by the presence of thick Moyie sills and competent siliceous beds in the metasediments. Deformation within the transition zone appears to have been partitioned between ductile cleaved semipelitic units and more rigid siliceous beds. As a result, relict sedimentary features in siliceous beds are locally preserved in the upper parts of the transition zone even though more argillaceous layers are strongly deformed. Semipelitic metasediments above and below Moyie sills in the transition zone are platy and porcelain-like, but the sills preserve their massive character. The porcelain-like character of these rocks appears to be a result of a dramatic decrease in grain size (0.1–0.5 mm) compared to the typical Lower Aldridge formation metasediments (1–4 mm). Rare porphyroclasts of altered feldspar in the transition zone metasediments suggest that this decrease in grain size may be related to grain-size reduction by dynamic recrystallization during deformation.

Relict mylonitic fabrics are also locally preserved in the upper parts of the transition zone, although the affects of late recrystallization have obscured key kinematic indicators. The lower contact of one thick sill within the transition zone south of the St. Mary River displays a mylonitic fabric defined by plagioclase porphyroclasts with asymmetric pressure fringes set in a matrix of fine-grained Fe-Mg chlorite (Fig. 7). A gradual increase in muscovite grain size in semipelitic layers through the transition zone results in increasingly friable and schistose rocks near the contact with the core zone. The coincidence of sericitic alteration of metasediments, chloritization of Moyie sills, and mylonitic fabrics within the transition zone suggests that fluids may have played an important role during deformation.

Metamorphic mineral assemblages and textures also change markedly going down through the transition zone. Garnetiferous schist first appears near the bottom of the transition zone, where $S_0 = S_1$, and becomes increasingly coarse grained at deeper structural levels. Alteration of garnet and biotite to greenish Fe-Mg chlorite is widespread in these rocks. Sillimanite first appears roughly 20 m below the first appearance of garnet and is ubiquitous as one proceeds to deeper levels.

Structural features

Geometry of the Matthew Creek metamorphic zone

The lack of outcrop in the St. Mary River valley makes it impossible to unequivocally establish the continuity of structural features across the MCMZ. Nonetheless, those areas that have been mapped share structural and metamorphic similarities that strongly suggest that the MCMZ is continuous across the St. Mary River valley.

Two distinct deformational events, D_1 and D_2, have affected the rocks of the MCMZ. D_1 fabrics include the shallowly dipping layer-parallel S_1 schistosity and L_1 mineral lineation and tight recumbent folds and boudinaged pegmatites in the core zone. Upright D_2 open folds and steep east–west- and north–south-trending brittle faults overprint D_1 fabrics. These D_2 fabrics are similar in style and orientation to structures throughout the Purcell Anticlinorium that formed during the Mesozoic through Tertiary (Price 1984).

Upright arching of the Lower Aldridge formation at this structural level has allowed the core zone to crop out in a dome. The general geometry of this dome is reflected by the outcrop pattern of Moyie sills in the regional-grade Lower Aldridge formation metasediments surrounding the MCMZ. The transition from low-grade Lower Aldridge formation metasediments to core zone schists has well-defined boundaries on the southern, eastern, and western margins of the structure. The transition in the north is ill defined, because

Fig. 6. (A) Boudinaged quartz(Qtz)-rich pegmatites in the core zone. Photo is taken roughly normal to northeast–southwest sillimanite lineation. (B) Detail of upper contact of lower boudin set in (A) above. Light layers are siliceous sedimentary layering (S_0) that has been tightly folded with F_1 roughly parallel to $S_1 = S_0$. Fold asymmetry suggests dextral shear sense. Brown tourmaline (Tur) defines the darker layers that appear to have deformed in a more ductile fashion, as suggested by the apparent flow of these layers into hinge regions.

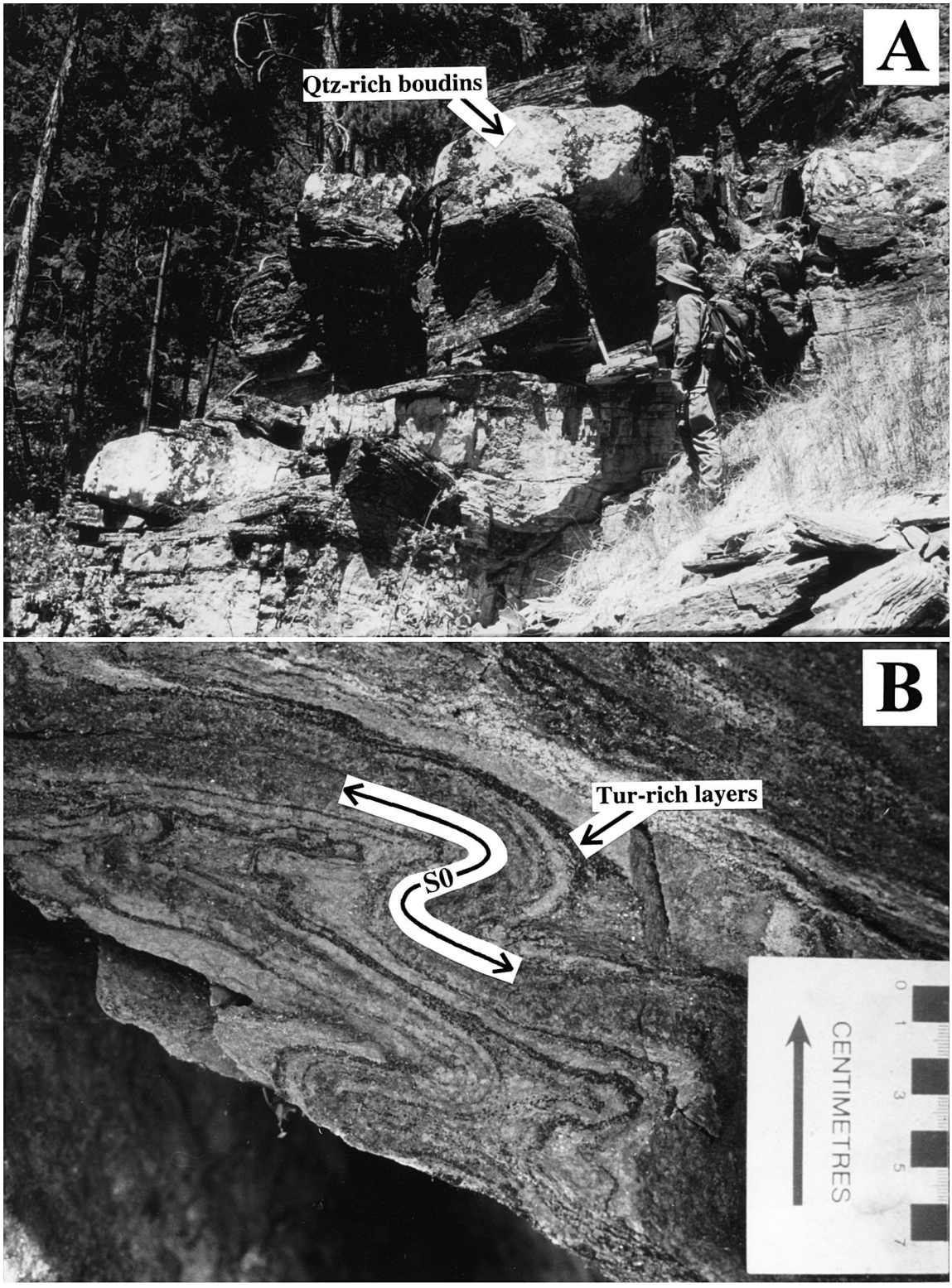

Fig. 7. Mylonitized Moyie sill from the southern portion of the MCMZ. Thin section is cut perpendicular to S_1 and parallel to L_1 with northeast to the right. The dominant S-surface slopes downward from upper right to lower left and is cut by a shallow C-surface (in upper right and lower left corners) that slopes from upper left to lower right. The orientation of S_0 in metasedimentary layering immediately below this sill is also shown. The sense of shear is top-to-the-right. Chl, chlorite; Pl, plagioclase.

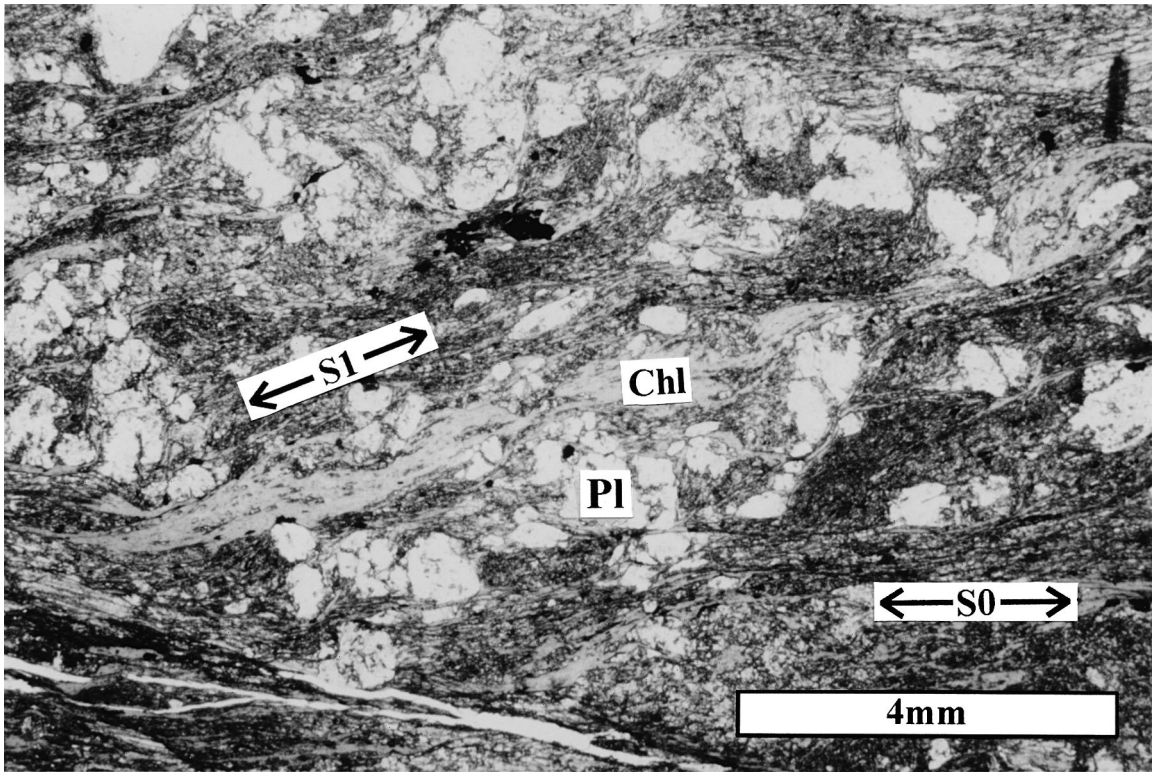

of poor exposure. However, constraints on its shape and extent in the north are provided by limited subsurface data. A 1000 feet vertical diamond drill hole was collared by Sedex Mining Inc., ~900 m north of the inferred extent of the core zone (see Fig. 2). The rock encountered for the entire length of the drill hole was continuous thinly bedded regional-grade Lower Aldridge formation rocks. These data indicate that the core zone is either faulted off or dips steeply (>40°) below the regional-grade rocks on its northern margin.

Regional structures

Steeply dipping brittle faults and upright east-vergent shallowly plunging folds overprint the earlier formed D_1 ductile features. Figure 8A shows poles to measurements of axial planes for minor D_2 folds and D_2 crenulation cleavages for the entire MCMZ and F_2 hinge lines for minor upright folds for the northern and southern portions of the MCMZ. Axial plane orientations were measured in the field when the geometry of the fold was well enough exposed to identify the trend and plunge of fold-hinge lines and the dip of the axial surface. These data have been contoured to highlight the cluster of points that define a mean axial surface of 163/66. Hinges of minor folds in the northern portion plunge to the north-northeast, while minor folds in the southern portion plunge to the south-southeast. F_2 hinge lines display a wide scatter that may be attributable to some or all of uncertainties arising from measuring hinge lines in vertical faces, real local variations arising from lithological heterogeneity, and possible inclusion of unresolved F_1 minor folds. The scatter may also be the result of east-vergent folding during east-directed Mesozoic contraction followed by north-northwest – south-southeast imbrication on the northern panel of the doubly plunging Moyie Anticline that may be responsible for late arching of the structure about an axis roughly perpendicular to F_2 (see Fig. 1).

Brittle faults throughout the MCMZ display two dominant trends: roughly east–west and north–south. The faults zones display narrow 1–30 cm cataclastic crush zones and are locally flanked by shear folds. Displacements along these faults are difficult to constrain, and many appear to vanish along strike. The sense of movement along most of these faults is obscured by the poor exposure in the immediate fault zone, although shear folds adjacent to several larger faults allowed several north-trending normal and reverse faults to be mapped.

Core zone structures

Ductile D_1 deformation fabrics predominate in the core zone. Features such as ptygmatic and recumbent folding (cf. Fig. 6B.); gneissic banding with concordant quartz-feldspar lenses; flattened and rotated porphyroblasts; and symmetrically boudinaged pegmatites (cf. Fig. 6A) are common. Poles to S_1 for the entire MCMZ plot as a wide scattered girdle resulting from the doubly plunging nature of the fold. These data also indicate that S_1 predates D_2 folding (Fig. 8B). Some of the scatter reflects the influence of peg-

matitic pods and stocks that locally deflect the foliation throughout the core zone (see foliation measurements near Matthew Creek stock in Fig. 3).

L_1 mineral lineation measurements in the core zone, defined by elongate sillimanite crystals, plot in two distinct clusters. The southerly cluster plunges on average 16–214, whereas the northerly cluster plunges on average 18–036. These data are consistent with superposition of upright D_2 folding on a preexisting shallowly plunging, northeast – southwest-trending D_1 lineation. The growth of lineated sillimanite within S_1 foliation planes strongly suggests that deformation occurred at sillimanite-grade conditions.

Transition zone structures

Structures in the "transition zone" are transitional between those of the regional rocks and the core zone. The dominant structural features in the middle and lower parts of the transition zone are like those of the core zone, consisting of a platy foliation parallel to S_1 in the schist and a weak L_1 stretching lineation inferred to have formed during D_1 deformation. In thin section, semipelitic transition zone rocks are fine grained (0.1–0.5 mm) and equigranular with numerous triple junctions. Many transition zone samples contain fish-shaped biotites and lenses of polygonized quartz and untwinned plagioclase oriented parallel to S_1. The polygonized lenses may be relict quartz or plagioclase clasts that have been dynamically recrystallized during deformation within the transition zone. Together with the preservation of centimetre-scale plagioclase porphyroclasts set in the fine-grained matrix, these features suggest that the transition zone contains localized mylonite zones that have been overprinted by later static recrystallization. The intensity of all these features decreases as one approaches the overlying regional rocks.

Lack and ambiguity of kinematic indicators in the core zone and transition zone

Kinematic indicators in the transition zone and core zone are scarce and difficult to interpret. Although the strong lineation in the core zone and lower part of the transition zone indicates northeast – southwest-trending movement, we could not determine with any confidence whether the sense of movement between the overlying biotite-grade metasediments and underlying core-zone schist was top-to-the-NE or top-to-the-SW. Asymmetric pressure fringes on isolated porphyroblasts and asymmetrically folded layering in six outcrops in the northern half of the core zone give a top-to-the-NE sense of shear. Few kinematic indicators were identified in the southern half, and these yielded ambiguous results in oriented thin sections. Asymmetric pressure fringes on plagioclase porphyroclasts in relict mylonites from the lower contact of a thick sill in the transition zone in the southern half of the MCMZ (described above) are also most consistent with a top-to-the-NE sense of motion. Whether these isolated outcrop-scale data are representative of movement across the zone as a whole is uncertain, especially given the large gap in outcrop exposure in the St. Mary River Valley.

Metamorphic conditions

Mineral assemblages, mineral compositions, and textures were used to estimate peak *P–T* conditions and the *P–T* evolution of rocks in the regional-grade Lower Aldridge formation and core zone schist. The 194 samples throughout the area were examined in thin section. In addition, a transect along line C–C′ (Fig. 9) was sampled to explore the change in grade between these two domains. Although many of the rocks are heavily altered, minerals in 11 relatively unaltered metapelitic and 5 metabasic samples were analyzed using the ARL SEMQ 9-channel wavelength dispersive electron microprobe at the University of Calgary. Operating conditions, precision, and mineral standards are the same as DePaoli and Pattison (1995). Selected compositional data for biotite, muscovite, garnet, plagioclase, and ilmenite for

Fig. 8. Equal area projections from the lower hemisphere of D_1 and D_2 structural fabrics in the MCMZ. (A) Poles to axial planes and F_2 fold axes to minor folds throughout the MCMZ. Axial planes were measured for upright open minor folds in siliceous ribs and for chevron-style crenulations. Fold axes for the northern and southern portions of the MCMZ (i.e., north and south of the St. Mary River) have been plotted separately to highlight the overall doubly plunging nature of the major anticlinal structure. (B) Poles to S_1 foliations and L_1 mineral lineations. Poles to S_1 plot as a wide dispersed girdle resulting from the doubly plunging nature of the D_2 arching. L_1 lineations are plotted for the northern and southern portions of the field area. They define two clusters distributed symmetrically on either side of the S_1 girdle suggesting they have been folded along with S_1 by later D_2 structures. Mean orientation data calculated as largest eigenvector of the distribution function. Mean great circles are normal to the mean orientation of the data. Contour intervals are calculated as the percentage of the distribution that falls within a circle of 1% radius over an equally spaced grid on the projection.

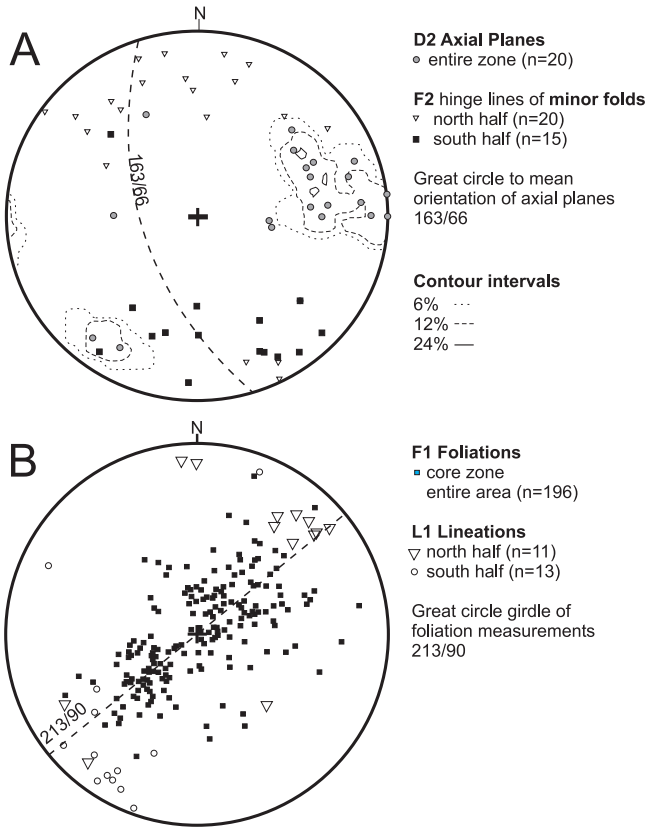

Fig. 9. Locations along cross section C–C′ of samples discussed in the text. See Fig. 3 for transect location. Lithologies and abbreviations as in Fig. 2.

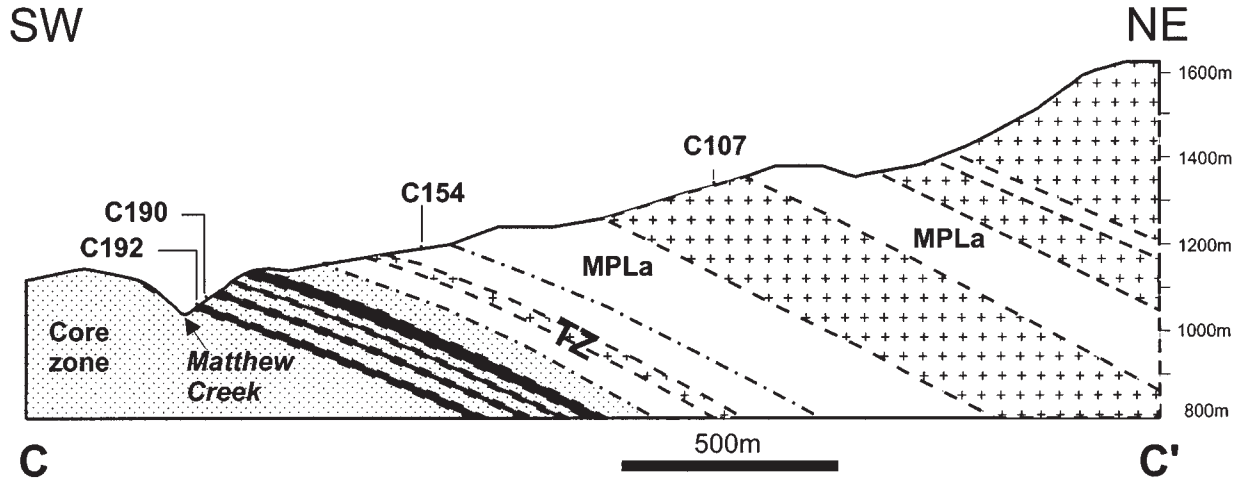

metapelitic samples are given in Table 1. Data for hornblende, plagioclase, epidote, titanite, and ilmenite in metabasic samples are given in Table 2.

Regional-grade metasediments

Metapelites

Estimating pressure and temperature conditions in the surrounding Lower Aldridge formation metasediments is problematic, due to the lack of diagnostic metamorphic assemblages in these siliceous metasediments. The two most common mineral assemblages are Ms–Bt–Qtz–Pl and Ms–Bt–Pl–Kfs–Qtz. Both of these assemblages are stable from conditions of the biotite isograd (ca. 400–450°C) to the Ms + Qtz–breakdown (600–650°C) (see Fig. 10).

The *P–T* estimates of DePaoli and Pattison (1995) of 450 ± 50°C and 3.8 ± 1 kbar for metamorphism of anomalously Mn-rich garnet-bearing metasediments in the Sullivan Mine probably represent a lower limit for *P–T* conditions of the Lower Aldridge formation immediately above the MCMZ. The Sullivan Mine is structurally ~1.5 km above the MCMZ, so that conditions closer to 500°C (assuming a steady state crustal geotherm of 30°C·km^{-1}) may be a reasonable estimate, consistent with scattered garnet reported in Lower Aldridge formation rocks in the general vicinity (Berry 1951; D. Brown, personal communication, 1997)

Metabasites

Regional metamorphic conditions in the surrounding rocks can also be constrained by the mineralogy of the Moyie sills. Green Ca-amphiboles were analyzed in samples C107 and C003. These are ferro- to magnesio-hornblendes that contain ~10 wt.% Al_2O_3, 1.2% CaO + K_2O, and 0.25%TiO_2. The hornblende in C003 coexists with a range of plagioclase compositions between An_{05} and An_{40}, while in C107 concentrically zoned plagioclase is ~An_{55} and is probably of partial igneous origin. Both samples contain minor epidote, chlorite, and a calcic white mica, but lack ilmenite. Although both samples contain minerals typically found in greenschist-facies metabasites (Ep, Chl, white-mica), the presence of green hornblende rather than actinolite and plagioclase of $An_{>20}$ is indicative of the epidote–amphibolite facies in metabasites (Spear 1993). Bégin and Carmichael (1992) identified the transition from greenschist- to amphibolite-facies metabasites in the Cape Smith Belt of northern Quebec, on the basis of the transition from actinolite + albite to hornblende + oligoclase. Although the presence of Ab-rich Pl in C003 ostensibly suggests that the rocks were down-grade of the Bégin and Carmichael (1992) hornblende + oligoclase isograd, given the evidence for late retrogression in the surrounding rocks (see below), it is difficult to be sure that the albite was stable with the rest of the assemblage. The absence of actinolite-intergrowths with hornblende in any of the metabasites that intrude the Lower Aldridge formation at this level suggests that temperatures were greater than Bégin and Carmichael's actinolite + albite-out curve at ~525°C, but the temperature estimate for this reaction is poorly constrained and subject to compositional variability. Uncertainties in the phase equilibria do not allow meaningful pressures to be estimated from metabasites in the immediate periphery of the MCMZ, although the minimum pressure for the epidote–amphibolite facies is about 3 kbar (Spear 1993, p. 408).

In summary, metapelitic and metabasic mineral assemblages in the overlying metasediments loosely constrain temperatures and pressures to approximately 450–500°C and ~4.0 kbar.

Core zone rocks

High-grade metapelites

The prograde *P–T* path and peak metamorphic conditions for the core zone can be constrained by several mineralogical and textural criteria in metapelitic schists. The calibrated metapelitic grid of Pattison and Tracy (1991, pp. 165–173) and multiequilibrium–multispecies thermobarometry estimates using TWEEQU1.02 (Berman 1991) and INVEQU (Gordon 1992), have been used to constrain pressure–temperature conditions. M_1 metamorphism in the core zone is recorded by a range of mineralogical and textural associations in high-grade schists containing the assemblage Ms–Bt–Qtz–Pl ± Grt ± Sil or And ± St. The M_1 metamorphic history is summarized by the *P–T* path in Fig. 10. The earli-

Table 1. Selected average mineral compositions from regional-grade and core zone metapelites.

	C154 – Lower Aldridge formation metasediment				C190 – Core-zone schist						
	Ms–Bt–Pl–Qtz				Ms–Bt–Grt–Pl–Qz–Sil–Ilm						
	Ms	Bt	Pl		Grt			Bt		Pl	Ms
			(Ab)	(Olig)	Core	Adj. Qtz	Adj. Bt	Core	Adj. Grt		
SiO_2 (wt.%)	47.23	37.94	67.32	62.38	36.11	35.96	36.14	36.29	35.56	62.71	47.27
TiO_2	1.08	1.80	0.01	0.01	bdl	bdl	bdl	1.81	1.85	—	0.42
Al_2O_3	32.48	17.10	20.55	23.77	20.69	20.70	20.78	19.85	19.54	23.12	36.17
FeO	1.19	15.51	0.08	0.07	38.13	38.53	38.73	23.11	22.86	0.10	0.83
MnO	—	—	—	—	1.42	1.07	1.06	0.04	0.03	—	0.01
MgO	1.55	13.38	0.02	0.00	1.86	1.79	1.63	7.77	7.83	0.01	0.45
CaO	0.01	0.01	1.04	4.87	1.19	1.09	1.09	0.01	0.04	3.88	0.06
Na_2O	0.27	0.02	10.99	8.84	bdl	bdl	bdl	0.11	0.12	9.07	1.19
K_2O	10.66	9.51	0.23	0.26	—	—	—	8.14	8.45	0.32	9.04
BaO	—	—	—	—	—	—	—	0.05	0.04	bdl	0.17
F	0.08	0.68	0.02	0.01	0.06	0.05	0.11	0.47	0.48	0.03	0.10
Total	94.55	95.95	100.20	100.22	99.46	99.18	99.55	97.66	96.80	99.23	95.71
Cations											
Si	6.33	5.57	11.77	11.04	5.93	5.93	5.93	5.39	5.35	11.17	6.75
Ti	0.22	0.4	0.00	0.00	—	—	0.00	0.41	0.42	—	0.09
Al	5.13	2.96	4.23	4.96	4.00	4.02	4.02	3.47	3.46	4.85	6.09
Fe	0.13	1.90	0.01	0.01	5.24	5.31	5.31	2.87	2.87	0.01	0.10
Mn	—	—	—	—	0.20	0.15	15.00	0.01	0.00	—	0.00
Mg	0.31	2.93	0.00	0.00	0.46	0.44	0.40	1.72	1.75	0.00	0.10
Ca	0.00	0	0.20	0.92	0.21	0.19	0.19	0.00	0.01	0.74	0.01
K	0.07	0.01	3.72	3.03	0.00	0.00	0.00	0.03	0.03	3.13	0.33
Na	1.82	1.78	0.05	0.06	—	—	—	1.54	1.62	0.07	1.65
Ba	—	—	—	—	—	—	—	0.00	0.00	0.00	0.01
F	0.01	0.09	0.01	0.01	0.03	0.02	0.06	0.06	0.06	0.02	0.03
Total	14.03	15.62	20.00	20.03	16.07	16.06	16.06	15.50	15.58	20.00	15.14
Mg/Mg + Fe	0.70	0.61			0.08	0.08	0.07	0.37	0.38		
			X_{Ca} = 0.049	X_{Ca} = 0.23	X_{alm} = 0.86	0.87	0.88			X_{Ca} = 0.19	
			X_{Na} = 0.94	X_{Na} = 0.76	X_{prp} = 0.075	0.07	0.07			X_{Na} = 0.79	
			X_K = 0.0129	X_K = 0.01	X_{grs} = 0.03	0.03	0.03			X_K = 0.02	
					X_{sps} = 0.034	0.03	0.03				

Note: bdl, below detection limit; —, did not analyze. Cation calculation basis: Ms/Bt 22 O, Grt 28 O, Pl 32 O, Hbl 23 O, Czo 8 cations, Ttn 4 Si, Ilm 6 cations. Total Fe in Bt, Grt assumed as Fe^{2+}. Fe^{3+} estimates in Hbl after Richard and Barrie (1990) and in Czo and Ttn after Schumacher (1991).

Table 2. Selected average mineral compositions from regional-grade and core zone metabasites.

	C107 – typical amphibolitized Moyie sill					C192 – Core zone mafic gneiss							
	Hbl–Pl–Czo–Ttn–Qtz					Hbl–Pl–Czo–Bt–Ilm–Ttn							
	Hbl	Czo	Pl		Ttn	Hbl	Pl		Czo	Ilm	Ttn	Bt	
			(Core)	(Rim)			Core	Rim				Core	Rim
SiO_2 (wt.%)	47.19	41.04	52.82	54.04	31.75	41.91	54.77	56.37	40.54	bdl	31.77	36.75	37.18
TiO_2	0.25	0.03	—	—	38.56	0.73	—	—	0.03	53.42	38.22	2.68	2.37
Al_2O_3	10.24	30.13	29.76	28.50	2.53	15.33	27.91	27.29	31.73	bdl	3.31	16.73	16.56
FeO	18.19	6.82	0.06	0.11	0.32	22.58	0.10	0.29	5.80	44.48	0.44	25.40	24.78
MnO	0.35	0.08	—	—	0.03	0.32	—	—	0.08	1.71	0.05	0.14	0.11
MgO	9.09	0.01	bdl	bdl	bdl	4.93	bdl	0.01	0.01	0.13	bdl	7.18	7.47
CaO	12.27	23.63	12.21	10.84	27.44	11.71	10.37	9.33	23.75	0.10	27.51	0.09	0.22
Na_2O	0.78	bdl	4.97	5.83	bdl	1.13	6.21	6.91	bdl	bdl	bdl	0.03	0.01
K_2O	0.43	—	0.06	0.05	—	0.88	0.06	0.08	—	—	—	9.13	4.76
BaO	bdl	—	bdl	bdl	—	bdl	—	—	—	—	—	—	—
F	0.07	bdl	0.03	0.01	0.37	0.12	0.02	0.01	0.44	0	0.44	0.24	0.28
Total	98.86	101.74	99.91	99.38	101.00	99.65	99.43	100.3	101.74	99.9	101.74	98.38	93.74
= -O = Cl,F	0.03					0.05							
Total	98.83					99.59							
Cations													
Si	6.95	3.05	9.59	9.82	4.00	6.29	9.95	10.13	2.99	0.00	4.00	6.05	6.27
Ti	0.03	0.00	—	—	3.65	0.08	—	—	0.00	4.04	3.62	0.66	0.60
Al	1.78	2.64	6.37	6.12	0.38	2.71	5.98	5.78	2.76	0.00	0.49	3.24	3.27
Fe^{2+}	2.15	0.15	0.01	0.02	0.03	2.63	0.02	0.04	0.13	1.87	0.05	3.49	3.47
Fe^{3+}	0.08	0.27	—	—	—	0.21	—	—	0.23	—	—	—	—
Mn	0.04	0.01	—	—	0.00	0.04	—	—	0.01	0.1	0.00	0.02	0.02
Mg	1.99	0.00	0.00	0.00	0.00	1.10	0.00	0.00	0.00	0.01	0.00	1.76	1.87
Ca	1.94	1.88	2.38	2.13	3.70	1.88	2.02	1.80	1.88	0.01	3.71	0.02	0.04
Na	0.22	0.00	1.75	2.04	0.00	0.33	2.19	2.41	0.00	0.00	0.00	0.01	0.00
K	0.08	0.00	0.01	0.01	—	0.17	0.01	0.02	—	—	—	1.92	1.02
Ba	—	—	—	0.00	—	—	—	—	—	—	—	—	—
F	0.03	0.00	0.02	0.01	0.15	0.06	0.01	0.01	0.00	0.01	0.18	3.00	0.04
Total	15.30	8.00	20.11	20.15	11.92	15.49	20.17	20.19	8.00	6.00	12.04	17.20	16.58
Mg/Mg + Fe	0.48					0.42				X_{Fe} = 0.96		0.34	0.35
			X_{Ca} = 0.57	0.51			X_{Ca} = 0.48	0.43		X_{Mg} = 0.01			
			X_{Na} = 0.42	0.49			X_{Na} = 0.52	0.57		X_{Mn} = 0.04			
			X_K = 0.00	0.00			X_K = 0.00	0.00					

Note: bdl, below detection limit; —, did not analyze. Cation calculation basis: Ms/Bt 22 O, Grt 28 O, Pl 32 O, Hbl 23 O, Czo 8 cations, Ttn 4 Si, Ilm 6 cations. Total Fe in Bt, Grt assumed as Fe^{2+}. Fe^{3+} estimates in Hbl after Richard and Barrie (1990) and in Czo and Ttn after Schumacher (1991).

Fig. 10. *P–T* diagram for KFMASH pelites modified from Pattison and Tracy (1991). The arrow labelled (*a*), (*b*), and (*c*) corresponds to the evolution of a high-grade core-zone schist sample. Dark grey area represents maximum *P–T* conditions of the core-zone schist with respect to the Pattison (1992) triple point (P). The position of the Holdaway and Mukhopadhyay (1993) triple point (H) extends the range of possible *P–T* conditions to lower temperatures and pressures indicated by the light grey region. These lower pressures are inconsistent with estimates of 3.8 ± 1 kbar based on silicate–carbonate equilibria using the thermodynamic database of Berman (1991) (which gives a triple point of 505°C and 3.75 kbar) at the nearby Sullivan Mine (DePaoli and Pattison 1995). The dashed curve shows the effect on the wet-melting curve of an addition of 2% by molar volume of B_2O_5 to the fluid phase. The resultant reduction of P_{H2O} would shift the wet-melting curve to lower temperatures approaching the conditions recorded by the high-grade schist. Kfs + Chl breakdown from Spear (1993) (S,93) and Bucher and Frey (1994) (B&F,94 curve). Position of wet-melting curve from Thompson and Algor (1977).

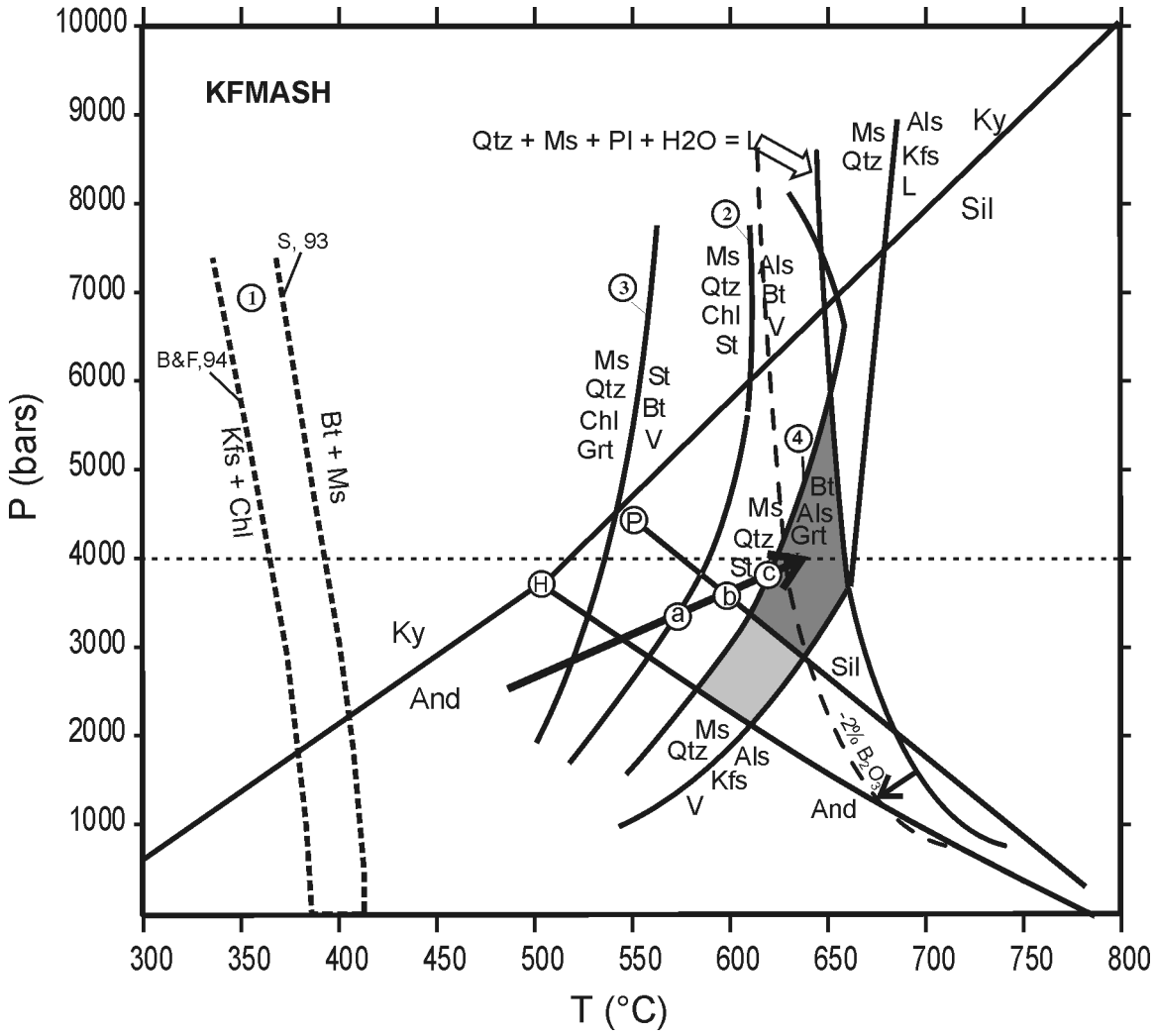

est stage of M_1 metamorphism involved prograde growth of Bt_1, Mn-rich Grt_1, and St_1, all of which are commonly included in large (locally 30 cm long) And_1 porphyroblasts (Fig. 11A). The andalusite crystals are oriented randomly within foliation planes, and Bt_1 crystals generally have cleavages set at a high angle to S_1. Grt_1 forms subhedral grains surrounded by quartz-rich pressure shadows. Ignoring the presence of the Mn-rich Grt_1, the minimum stability of Ms + Al_2SiO_5 + Bt_1 is given by the model reaction

$$\text{Ms + Chl + St + Qtz} = \text{And + Bt + } H_2O \text{ (reaction [2] in Fig. 10)}$$

(represented by assemblage "a" in Fig. 10), which is consistent with the presence of inclusions of St_1 within And_1. Optically continuous Sil_1 in And_1 (basal sillimanite shown in Fig.11C) parallel to the length of the andalusite crystals indicates that And_1 was pseudomorphed by Sil_1 parallel to the And_1 c-axis. This suggests that static heating persisted into the sillimanite stability field (assemblage "b" in Fig. 10). The incorporation of St_1 in And_1 prior to the And–Sil transition limits pressures to <4 kbar on the Pattison and Tracy (1991) grid. At the later stages of M_1 metamorphism, ductile deformation, D_1, affected the rocks at sillimanite grade conditions as revealed by lineated (but not dismembered) Sil_1 in the matrix and wrapping of the S_1 foliation around And_1 and Grt_1 porphyroblasts. We interpret the strong ductile fabrics seen in the core zone to have been developed at this time.

The highest grade of M_1 metamorphism is represented by the assemblage Sil_1–Ms_1–Bt_2–Pl_1 (An_{25})–Alm Grt_2 (assem-

Fig. 11. Photomicrographs of important mineral assemblages and textures. (A) Large And_1 porphyroblast (portion of chiastolite cross partly visible) with inclusions of fractured and partly altered St_1 and fresh Bt_1. And_1 is also partially altered to a fine-grained white mica along cleavage planes. (B) Typical pelitic core zone schist with large equant Grt_1 with inclusion-rich cores and rims (Grt_2 overgrowth?), which locally include Sil_1. Skeletal Bt_1 is also present and is overprinted by Sil_1 and Ms_2. Both Grt_1 and Bt_1 show quartz-rich pressure shadows and are set in a matrix defined by Bt_2, Ms_1, Sil_1, Qtz, and locally Pl. (C) Photograph of the outer margin of a pseudomorph of Ms_2 after And_1 showing optically continuous Sil_1 basal sections preserved within the pseudomorph. Grt_1 on the periphery of the former And_1 porphyroblasts is retrogressed to a mixture of chlorite (Chl) + sericite (Ser). This altered Grt_1 and the outer portions of the pseudomorph are overprinted by idioblastic chloritoid (Cld) that is oriented perpendicular to the S_1 foliation. (D) Bt–Ms–Pl–Qtz schist with large pseudomorph. Grt_3 is visible as tiny idioblasts that overprint all preexisting fabrics.

blage "c" in Fig. 10). This assemblage plots upgrade of curve

$$Ms + St + Qtz = Grt + Sil + Bt + H_2O \text{ (reaction [4] in Fig. 10)}$$

and downgrade of

$$Ms + Qtz = Kfs + Sil + (H_2O \text{ or Liquid})$$

The presence of lineated Sil_1 in the margins of Grt_2 (Fig. 11B) may provide evidence for growth of Grt_2 on preexisting Grt_1 via reaction [4].

The occurrence of sparse leucocratic Pl + Qtz ± Ms segregations in the structurally lowest schists in the MCMZ suggest that *P–T* conditions were close to the water saturated melting curve (Ms + Pl + Qtz + H_2O = L). Pressures at these conditions must have been above the intersection of the Ms + Qtz breakdown curve and the And = Sil univariant curve (>2.5–3.0 kbar depending on which And = Sil curve is used) and most likely were below the triple point (<3.75–4.5 kbar). This latter constraint is based on the inferred sequence of reactions described above and a *P–T* path that is assumed to be approximately isobaric, as concluded by De Yoreo et al. (1991) in their compilation and thermal modelling of low pressure – high temperature metamorphism. Near-peak *P–T* conditions can, therefore, be constrained to a small polygon within a temperature range of 600–650°C and a pressure range of 3.0–4.5 kbar on the grid of Pattison and Tracy (1991) (or 2.5–4.0 kbar if the Holdaway and Mukhopadhyay (1993) triple point is used).

Multiequilibrium *P–T* estimates for the peak M_1 assemblage (509–531°C) are significantly lower than these petrogenetic grid estimates. The calculated effects of minor components cannot reconcile this disparity. A more likely explanation is either incorrect selection of parts of minerals that were in equilibrium at peak conditions, or variable resetting of the mineral compositions following peak conditions (for example, there is textural evidence for several generations of garnet, biotite and muscovite growth). For these reasons, we favour the petrogenetic grid *P–T* estimates.

M_1 mineral assemblages are overprinted by a second metamorphism that resulted in the partial to complete replacement of And_1 and variable replacement of M_1 Grt_1 by coarse, randomly oriented Chl_2 and especially Ms_2 (margarite also occurs locally in cores of And_1) (Fig. 11C). The source of the fluid to drive this hydration event and the timing of its infiltration are unconstrained. Muscovitization must postdate D_1 deformation, because randomly oriented Ms_2 aggregates would not be expected to survive the intense deformation recorded in the matrix of the schist.

A third metamorphic event resulted in the growth of idioblastic Grt_3 and locally Fe-rich chloritoid (visible in Fig. 11C) under static conditions. These minerals overprint all preexisting fabrics, including the Ms_2-rich pseudomorphs (Fig. 11D). *P–T* conditions of this event can be loosely constrained to 425–500°C based on the Cld–Grt–Bt assemblage (*see* Fig. 10-9, Spear 1993). The age of this metamorphism is also unknown, but conceivably may be related to the 1010–1050 Ma metamorphic ages reported by Anderson and Davis (1995). The final metamorphic episode involved local chloritization of $Bt_{1,2}$ and $Grt_{1,2}$ in metapelites and formation of chlorite after Hbl_1 and epidote after Bt_1 in metabasites.

A final deformation episode, D_2, is represented by the broad doming that exposes the MCMZ and an associated crenulation. These structures affect all preexisting fabrics, D_1, and all three metamorphic events. D_2 structures occur throughout the surrounding Lower Aldridge formation, the transition zone, and the core zone, and are most likely associated with Cordilleran eastward compression and regional shortening.

Metamorphic contrast between overlying rocks and core zone

Peak temperature in the Lower Aldridge formation in the immediate vicinity of the MCMZ has been loosely constrained to lie between 450 and 650°C with a best estimate of ~500°C. The best estimate of pressure is about 4 kbar. Peak *P–T* conditions for the core zone schist are constrained to the range 580–650°C at 3–4 kbar. The structural relief along the sample transect is 830 m. The apparent metamorphic gradient through this section is, therefore, between ~100°C·km^{-1} and 180°C·km^{-1}, far in excess of any known steady-state crustal gradient (avg. 25–30°C·km^{-1}). Coupled with the structural features, this anomalously steep thermal gradient suggests that a tectonic boundary, namely a ductile shear zone, separates the core zone from the regionally metamorphosed Lower Aldridge formation metasediments in the area.

Age of metamorphism and ductile deformation

A geochronological estimate for rocks of the MCMZ comes from metamorphic monazite grains from Ms–Grt–Sil–Bt schist near the mouth of Matthew Creek. Five fractions yielded <2% discordant $^{207}Pb/^{206}Pb$ ages in the range 1341 ± 1.1 to 1352 ± 1.1 Ma (Anderson and Parrish[2]). This age may

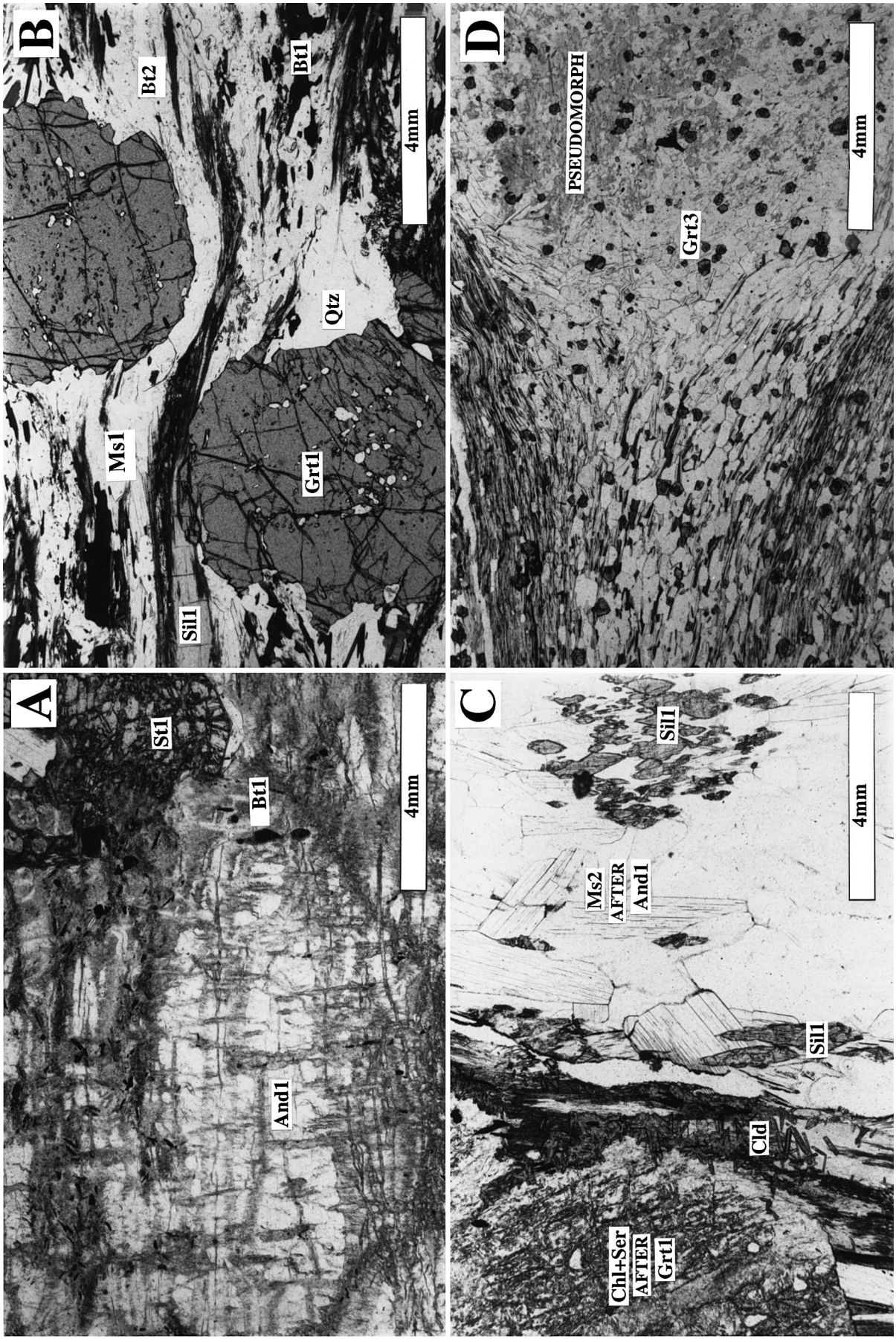

either record the time of metamorphic growth of the monazite (presumed to be due to the M_1 metamorphism that resulted in the high-grade mineral assemblage) or be a cooling age that would, therefore, represent a minimum age for the metamorphism. The two possibilities are difficult to distinguish, owing to the similarity of peak metamorphic temperatures (600–650°C) with estimates of the closure temperature of monazite (700°C, Heaman and Parrish 1991). However, a study of monazite growth by Crowley and Ghent (1999) found no evidence for Pb diffusion in inherited cores of monazite grains from rocks that experienced 650–700°C temperatures, suggesting that the monazite age from MCMZ is a formation age that represents the age of M_1 metamorphism.

Other lines of evidence give a broadly similar result. The Matthew Creek stock and all other pegmatitic sills in the core zone have deformed contacts against the high-grade schist, indicating that they were emplaced before or during the development of the D_1 deformation (and therefore M_1 metamorphism). These pegmatites are mineralogically and texturally indistinguishable from the 1365 ± 3 Ma (J. Mortensen, unpublished data) Hellroaring Creek stock and are likely of similar age. D_1 deformation and M_1 metamorphism would thus be about 1365 Ma or younger. An apparent contradiction to this interpretation is the reported truncation of a metamorphic foliation by the Hellroaring Creek Stock (Ryan and Blenkinsop 1971) 10 km SW of the MCMZ, suggesting a metamorphic-deformation event prior to the 1365 Ma age of the intrusion.

A cluster of titanite U–Pb ages around 1320–1370 Ma from the Sullivan orebody (Schandl et al. 1993), which DePaoli and Pattison (1995) correlated with peak metamorphism there, and a 1330 ± 45 Ma K–Ar age from metamorphic biotite from the Prichard formation of Idaho (equivalent to the Lower Aldridge formation in Canada) (Obradovich and Peterman 1968) provide further evidence for a ca. 1350 Ma metamorphism in the lower Purcell Supergroup. High-grade metamorphism in the Salmon River Arch of central Idaho at *ca*. 1370 Ma (Doughty and Chamberlain 1996) suggests metamorphism at this time may have been regional in extent. In summary, the age of M_1 metamorphism in the MCMZ and the accompanying formation of the L_1 sillimanite lineation and S_1 foliation can be constrained to 1341–1352 Ma with metamorphism affecting the lower Purcell and Belt supergroups sequence on a regional scale between 1300–1370 Ma.

Discussion

Cause of M_1 metamorphism

The progressive And–Sil series metamorphism documented in the high-grade schist requires anomalously high geothermal gradients, most likely due to the intrusion of igneous material (England and Thompson 1984). Although there is no clear geophysical or geological evidence for a nearby or underlying intrusion, the Matthew Creek metamorphic zone (MCMZ) lies near the thickest accumulation of Moyie sills in the Belt–Purcell Basin, interpreted by Höy et al.[2] to correspond to the rift axis of the basin. A possible source of magmatic heat to drive the And–Sil metamorphism may, therefore, have been intrusion of hot (>1000°C) mafic sills during renewed tectonic instability in the Belt–Purcell Basin at 1300–1370 Ma, recognizing that this implies a period of extension and mafic magmatism about 100 Ma later than the emplacement of the Moyie sills in the vicinity of the MCMZ.

One-dimensional heat conduction modelling shows that the intrusion of numerous thick mafic sills, with a cumulative thickness of 5 km under 15 km of crust, may be sufficient to raise temperatures isobarically by 100–150°C above ambient temperatures of 400–500°C (the latter assuming a thermal gradient of 30–40°C·km^{-1}). These temperatures would be sufficient to account for the growth of And–Sil assemblages and partial melting of pelitic material at the indicated pressures of 3–4 kbar. This interpretation is similar to that of Doughty and Chamberlain (1996), who suggested that high-grade metamorphism in the Yellowjacket basin of Idaho (equivalent to the Aldridge formation in southeastern British Columbia) occurred at 1370 ± 2 Ma coeval with mafic and felsic magmatism.

The numerous pegmatitic bodies (also dominantly sill-like) that crop out at deeper structural levels may represent high-level expressions of this magmatic activity. At about 650°C, partial melting may occur in rocks similar to the Lower Aldridge formation, which contain abundant quartz, feldspar, and micas by the "wet-melting" reaction Ms + Pl + Qtz ± Kfs + H_2O = L. This curve intersects the Ms + Qtz = Al_2SiO_5 + Kfs + H_2O dehydration reaction curve at an invariant point near 3.5–4.0 kbar, shown in Fig. 10. Freezing of anatectic melts formed by wet melting at pressures above this invariant point (the pressure estimate for the MCMZ schist is about 4 kbar) would yield granitoid rocks composed of Ms + Pl + Qtz ± Kfs, much like the pegmatitic rocks encountered in the field area. Small amounts of melt may have migrated a limited distance to crystallize as quartzofeldspathic bands, pods, and lenses, like those evident in rocks with gneissic banding at the deepest structural levels in the MCMZ. If enough in situ partial melting took place, the melt may have migrated upward to collect as larger masses like the Matthew Creek stock and the Hellroaring Creek stock.

The ubiquitous occurrence of tourmaline and beryl in the pegmatites suggests the presence of B_2O_3 may have depressed the wet-melting solidus, perhaps by as much as 50°C (Pichavant and Manning 1984; Pattison 1992), thereby approaching more closely the estimated *P–T* conditions of the schist (600–650°C). This interpretation is consistent with the absence of any local thermal metamorphism in the schist adjacent to the pegmatites, suggesting that the pegmatites were emplaced into host rocks of a similar temperature and were not the heat source for the M_1 metamorphism.

Nature and timing of the tectonic discontinuity at Matthew Creek metamorphic zone

In addition to causing an elevated thermal structure, intrusion of sill swarms during crustal extension may also have provided enough heat to cause localized, transient ductile regimes in the shallow crust (Lister and Baldwin 1993; Simony and Carr 1997), especially if anatexis were triggered. In an extensional setting, this might favour development of tectonic discontinuities (ductile shear zones) between schis-

tose, incipiently melting rocks, and the overlying more competent lower grade rocks.

This relationship is consistent with the relationships observed in the MCMZ. The presence of a package of thick, rigid mafic sills in the regional-grade metasediments immediately above the MCMZ would favour the development of ductile fabrics by localizing strain in the underlying pelitic rocks. These relatively impermeable sills may have also served to isolate rising metamorphic fluids derived from dehydration reactions at deeper structural levels. Rising fluids that reached the layer of relatively impermeable Moyie sills may have been concentrated along its base. This would result in higher fluid pressures accompanied by uralitization of pyroxenes or chloritization of hornblende in Moyie sills, and sericitization and phyllitization of metasediments. Higher fluid pressures would also tend to favour the development of localized mylonitic fabrics near or in the margins of Moyie sills by replacing feldspars with more easily deformed micas and quartz. It thus seems likely that the age of the ductile shearing between the core zone and the regionally metamorphosed Lower Aldridge formation rocks at Matthew Creek was about that of the D_1 deformation and M_1 metamorphism, ca. 1341–1352 Ma.

Without a more detailed structural analysis of the Matthew Creek metamorphic zone, we can only speculate on the sense of movement across the transition zone and the broader tectonic significance of the MCMZ in the mid-Proterozoic evolution of the Belt–Purcell supergroups sequence. Despite this uncertainty, the overall relationships exposed in the MCMZ are consistent with extension accompanied by anatexis in the deeper levels of the rifting Purcell Basin at about 1300–1370 Ma, leading to an elevated thermal regime and development of ductile detachments.

Acknowledgments

This work represents part of the M.Sc. thesis work of C.R.M.M. C.R.M.M. acknowledges financial assistance from the University of Calgary Department of Geology and Geophysics and the Belt Association Inc. Natural Sciences and Engineering Research Council of Canada Research Grant 037233 to David Pattison supported the field work. C.R.M.M. acknowledges the field assistance of J.B. Krauss. Both authors thank D. Brown, B. Woodfill, P. Ransom, and D. Anderson for their helpful discussions and input in this project and R.L. Brown, R.A. Price, M.J. Holdaway, and C.W. Dietsch who reviewed the paper.

References

Anderson, H.E., and Davis, D.W. 1995. U–Pb geochronology of the Moyie sills, Purcell Supergroup, southeastern British Columbia: implications for the geological history of the Purcell (Belt) basin. Canadian Journal of Earth Sciences, **32**: 1180–1193.

Anderson, H.E., and Parrish, R.R. 2000. U–Pb geochronological evidence for the geological history of the Purcell (Belt) basin. *In* The geological environment of the Sullivan Pb–Zn–Ag deposit, British Columbia. *Edited by* J.W. Lydon, J.F. Slack, T. Höy, and M. Knapp. MDD(GAC) – Geological Survey of Canada.

Bégin, N.J., and Carmichael, D.M. 1992. Textural and compositional relationships of Ca-amphiboles in metabasites of the Cape Smith Belt, northern Quebec: implications for a miscibility gap at medium pressures. Journal of Petrology, **33**: 1317–1343.

Berman, R.G. 1991. Thermobarometry using multi-equilibrium calculations: a new technique with petrological applications. The Canadian Mineralogist, **29**: 833–855.

Berry, A.D. 1951. A study of the Aldridge formation, St. Mary Lake area, British Columbia. M.Sc. thesis, The University of Alberta, Edmonton, Alta.

Bucher, K., and Frey, M. 1994. Petrogenesis of metamorphic rocks. 6th ed. Springer-Verlag, New York.

Crowley, J.L., and Ghent, E.D. 1999. An electron microprobe study of the U–Th–Pb systematics of metamorphosed monazite: the role of Pb diffusion versus overgrowth and recrystallization. Chemical Geology, **157**: 285–302.

DePaoli, G.R., and Pattison, D.R.M. 1995. Constraints on temperature-pressure conditions and fluid composition during metamorphism of the Sullivan orebody, Kimberley, British Columbia, from silicate-carbonate equilibria. Canadian Journal of Earth Sciences, **32**: 1937–1949.

De Yoreo, J.J., Lux, D.R., and Guidotti, C.V. 1991. Thermal modelling in low pressure/high temperature metamorphic belts. Tectonophysics, **188**: 209–238.

Doughty, P.T., and Chamberlain, K.R. 1996. Salmon River Arch revisited: new evidence for 1370 Ma rifting near the end of deposition of the Middle Proterozoic Belt basin. Canadian Journal of Earth Sciences, **33**: 1037–1052.

England, P.C., and Thompson, A.B. 1984. Pressure–temperature–time paths of region metamorphism, Part I: heat transfer during the evolution of regions of thickened continental crust. Journal of Petrology, **25**: 894–928.

Gordon, T.M. 1992. Generalized thermobarometry; solution of the inverse chemical equilibrium problem using data for individual species. Geochimica et Cosmochimica Acta, **56**: 1793–1800.

Heaman, L., and Parrish, R. 1991. U–Pb geochronology of accessory minerals. *In* Applications of radiogenic isotope systems to problems in geology. *Edited by* L. Heaman and J.N. Ludden. Mineralogical Association of Canada, Short Course Handbook No. 19, pp. 59–102.

Holdaway, M.J., and Mukhopadhyay, B. 1993. A reevaluation of the stability relations of andalusite; thermochemical data and phase diagram for the aluminum silicates. American Mineralogist, **78**: 298–315.

Höy, T. 1989. The age, chemistry and tectonic setting of the Middle Proterozoic Moyie Sills, Purcell Supergroup, southeastern British Columbia. Canadian Journal of Earth Sciences, **26**: 2305–2317.

Höy, T., Anderson, D., Turner, R.J.W., and Leitch, C.H.B. 2000. Tectonic, magmatic and metallogenic history of the early synrift phase of the Purcell basin, southeastern British Columbia. *In* The Sullivan deposit and its geological environment. Pb–Zn–Ag deposit, British Columbia. *Edited by* J.W. Lydon, T. Höy, J.F. Slack, and M. Knapp. MDD(GAC) – Geological Survey of Canada.

Kretz, R. 1983. Symbols for rock-forming minerals. American Mineralogist, **68**: 277–279.

Leech, G.B. 1957. St. Mary Lake, Kootenay District, British Columbia (82F/9). Geological Survey of Canada, Map 15-1957.

Leech, G.B. 1962. Metamorphism and granite intrusions of Precambrian age in southeastern British Columbia. Geological Survey of Canada, Paper 62-13.

Leech, G.B., Lowdon, J.A., Stockwell, C.H., et al. 1963. Age determinations and geological studies. Geological Survey of Canada, Paper 63-17, p. 30.

Lister, G.S., and Baldwin, S.L. 1993. Plutonism and the origin of metamorphic core complexes. Geology, **21**: 607–610.

McMechan, M.E., and Price, R.A. 1982. Superimposed low-grade metamorphism in the Mount Fisher area, southeastern British Columbia – implications for the East Kootenay orogeny. Canadian Journal of Earth Sciences, **19**: 476–489.

Obradovich, J.D., and Peterman, Z.E. 1968. Geochronology of the Belt Series, Montana. Canadian Journal of Earth Sciences, **5**: 737–747.

Pattison, D.R.M. 1992. Stability of andalusite and sillimanite and the Al_2SiO_5 triple point: constraints from the Ballachulish aureole, Scotland. Journal of Geology, **100**: 423–446.

Pattison, D.R.M., and Tracy, R.J. 1991. Phase equilibria and thermobarometry of metapelites. *In* Contact metamorphism. *Edited by* D.M. Kerrick. Mineralogical Society of America Reviews in Mineralogy, **26**: 168.

Pichavant, M., and Manning, D. 1984. Petrogenesis of tourmaline granites and topaz granites: the contribution of experimental data. Physics of the Earth and Planetary Interiors, **35**: 31–50.

Price, R.A. 1984. Tectonic evolution of the Purcell (Belt) rocks of the southeastern Canadian Cordillera and adjacent parts of the United States. *In* The Belt. Montana Bureau of Mines and Geology, Special Publication 90, p. 47.

Rice, H.M.A. 1937. Cranbrook map-area, British Columbia. Geological Survey of Canada, Memoir 207.

Richard, L.R., and Barrie, C.D. 1990. AMPHIBOL; a program for calculating structural formulae and for classifying and plotting chemical analyses for amphiboles. American Mineralogist, **75**: 421–423.

Ryan, B.D., and Blenkinsop, J. 1971. Geology and geochronology of the Hellroaring Creek stock, British Columbia. Canadian Journal of Earth Sciences, **8**: 85–95.

Schandl, E.S., Davis, D.W., and Gorton, M.P. 1993. The Pb–Pb age of metamorphic titanite in the chlorite-pyrite altered footwall of the Sullivan Zn–Pb SEDEX deposit, B.C., and its relationship to the ore. Geological Association of Canada – Mineralogical Association of Canada, Programs with Abstracts, **18**: p. A93.

Schofield, S.J. 1915. Cranbrook map area. Geological Survey of Canada, Memoir 76.

Schumacher, J.C. 1991. Empirical ferric iron corrections; necessity, assumptions, and effects on selected geothermobarometers. Mineralogical Magazine, **55**: 3–18.

Sears, J.W., and Price, R.A. 1994. Large Scale clockwise thrust rotation of the southern Canadian and northern Montana Rockies about on Euler pole near Helena, Montana; evidence from tectonic inversion of the Belt Basin. Geological Society of America, Annual Meeting, Abstracts with Programs, **26**(7): 526.

Simony, P.S., and Carr, S.D. 1997. Large lateral ramps in the Eocene Valkyr shear zone: extensional ductile faulting controlled by plutonism in southern British Columbia. Journal of Structural Geology, **19**: 769–784.

Spear, F.S. 1993. Metamorphic phase equilibria and pressure–temperature–time paths. Mineralogical Society of America, Washington, D.C. Monograph Series 1.

Thompson, A.B., and Algor, J.R. 1977. Model systems for anatexis of pelitic rocks. Contributions to Mineralogy and Petrology, **63**: 247–269.

White, W.H. 1959. Cordilleran tectonics in British Columbia. American Association of Petroleum Geologists Bulletin, **43**: 60–100.